

Mechanical relaxation of 4 wt % Y_2O_3 - ZrO_2 tetragonal single crystals

M. OZAWA*, H. HASEGAWA

Toyota Central Research and Development Laboratories Inc., Nagakute, Aichi, 480-11, Japan

The mechanical relaxation was examined by a resonance piezoelectric method for a 3.5 wt % Y_2O_3 - ZrO_2 polycrystal and 4 wt % Y_2O_3 - ZrO_2 tetragonal single crystals with orientations in the $\langle 100 \rangle$ and $\langle 111 \rangle$ directions. The relaxation was observed for the $\langle 111 \rangle$ -oriented crystal, but not for the $\langle 100 \rangle$ -crystal. The results indicated that the relaxation was active only for the elastic compliance, s_{44} , and inactive for $(s_{11}-s_{12})$. The amplitude of the anelastic relaxation measured for the polycrystalline and the $\langle 111 \rangle$ -crystal body was $4.2 \times 10^{-12} \text{ m}^2 \text{ N}^{-1}$ and $6.7 \times 10^{-12} \text{ m}^2 \text{ N}^{-1}$, respectively. An observed broad relaxation peak suggested that complex processes exist even in single crystals.

1. Introduction

Fluorite-structured ZrO_2 doped with Y_2O_3 provides a useful material, e.g., for oxygen-ion conductors and toughened ceramics [1, 2]. Tetragonal ZrO_2 doped with a small amount of Y_2O_3 has a high toughness due to martensitic transformation from tetragonal to monoclinic symmetry. However, thermal ageing at 200 to 300 °C often induces a degeneration in mechanical performance, e.g. in strength and toughness [3]. Several investigators described an internal-friction peak at 200–300 °C for ZrO_2 polycrystals with a small amount of Y_2O_3 [4–8]. They showed a broadened relaxation peak associated with a thermally activated process. In previous works [8, 9], the examination of several ZrO_2 polycrystal samples led to direct evidence that the peak was induced by the relaxation of oxygen defects.

The measurement of internal friction and mechanical relaxation is useful in obtaining information on the behaviour of solutes or complexes with an elastic dipole in co-ordination compounds [10–13]. The dopants Y^{3+} substitute for Zr^{4+} and introduce oxygen vacancies (V_O) to compensate for their low charge. The introduction of trivalent cations produces one V_O for every Y_2O_3 and induces local structure including a ($Y_{Zr}V_O$) complex in the ZrO_2 lattice. However, no detailed discussion for such local defect structure could be described for ZrO_2 doped with Y_2O_3 because of the limitation of using polycrystalline bodies. In this study, mechanical relaxation of ZrO_2 single crystal is examined to discuss the symmetry of the defect complexes in fluorite-type oxides.

2. Experimental procedure

2.1. Sample

The experiments were carried out on both sintered polycrystalline ZrO_2 , containing 3.5 wt % Y_2O_3 (from Tosoh Corporation, Tokyo, Japan), and on single-

crystal ZrO_2 doped with 4 wt % Y_2O_3 (from Ceres Inc., USA). Samples were cut to a 3 × 4 mm cross-section and to a 25–30 mm length. Single-crystal samples were cut to prepare bars with the long axis oriented along $\langle 100 \rangle$ and $\langle 111 \rangle$, which were determined by a Laue pattern. Elastic measurement was performed for $\langle 100 \rangle$ - and $\langle 111 \rangle$ -oriented crystals. ZrO_2 has a maximum and minimum Young's modulus in the $\langle 100 \rangle$ and $\langle 111 \rangle$ directions, respectively. X-ray diffraction (XRD) examination revealed that samples consisted of tetragonal domains showing $(100)_t \parallel (001)_t$.

2.2. Elastic measurement

A piezoelectric resonance method was applied to composite bars of piezoelectric vibrators and samples [14, 15]. Quartz vibrators were -18.5° X-cut bar for longitudinal vibration at 90 to 140 kHz. A $LiNbO_3$ vibrator was also used for measurement at elevated temperatures, above 500 °C. The details of the measurement procedure have been described in previous papers [16, 17]. The internal-friction data were influenced by the difference in the resonance frequencies of the vibrators and samples, and were therefore calibrated by an experimental equation [9, 16]. The Young's modulus at elevated temperatures was calculated using the thermal-expansion data of ZrO_2 - Y_2O_3 crystals [18].

3. Results

3.1. Polycrystals

Fig. 1 shows the Young's modulus, E , and internal friction, Q^{-1} , plotted against temperature, T . The peak shows thermally activated relaxation with a relaxation strength $\Delta = 1.34 \pm 0.08 \times 10^{-2}$, an activation enthalpy $H = 82.5 \pm 1.4 \text{ kJ mol}^{-1}$ and a relaxation-time pre-exponential term $\tau_0 = 5.4 \pm 1.1 \times 10^{-14} \text{ s}$,

* Present address: Ceramics Research Laboratory, Nagoya Institute of Technology, Tajimi, Gifu, 507, Japan.

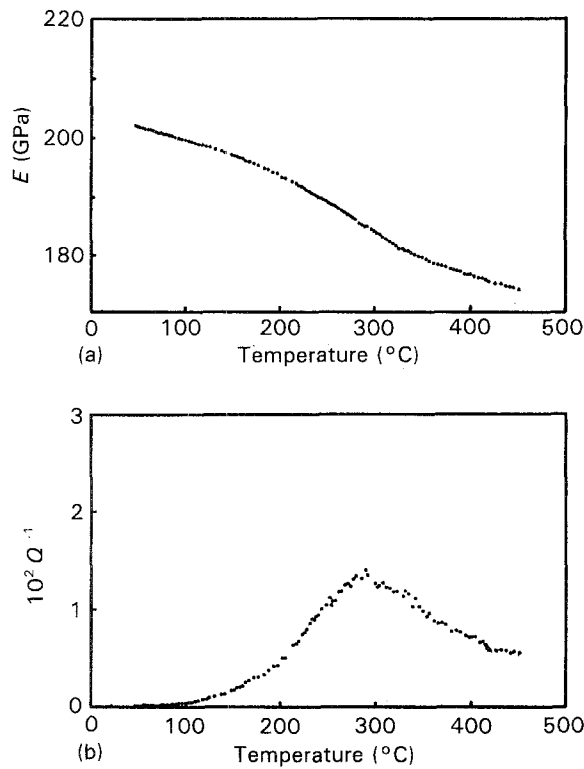


Figure 1 Temperature dependence of: (a) Young's modulus, E , and (b) internal friction, Q^{-1} , for polycrystalline 3.5 wt % Y_2O_3 - ZrO_2 .

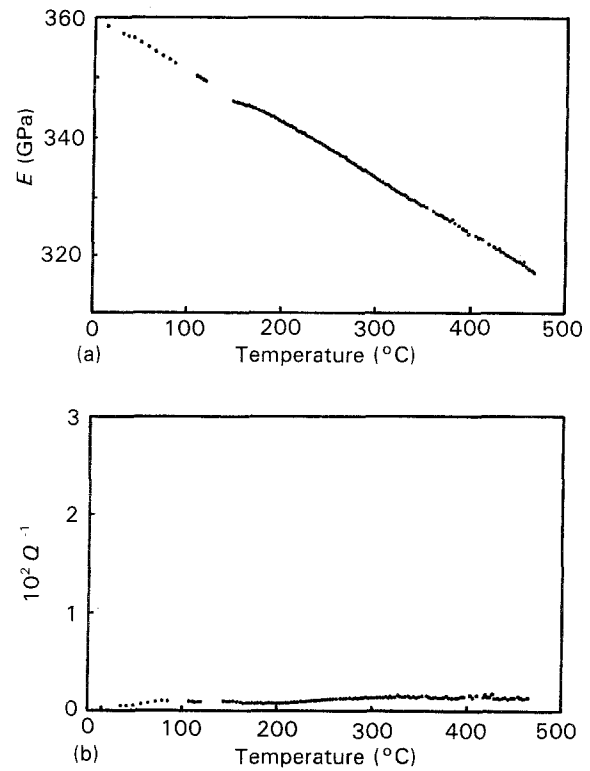


Figure 2 Temperature dependence of: (a) Young's modulus, E , and (b) internal friction, Q^{-1} , for a $\langle 100 \rangle$ -oriented 4 wt % Y_2O_3 - ZrO_2 crystal.

obtained from the relation between the frequency and peak temperature [9].

3.2. $\langle 100 \rangle$ -oriented crystals

Fig. 2 shows E and Q^{-1} measured for a crystal with a $\langle 100 \rangle$ orientation. As mentioned above, the crystal does not have a complete $\langle 100 \rangle$ orientation, but has mixed $\langle 100 \rangle$ and $\langle 001 \rangle$ orientations. Thus, the symmetry may practically be treated as a pseudo-cubic symmetry of ZrO_2 for the crystal used in the present study, because of its small tetragonality, $c/a = 1.015$. It should be noted that no internal-friction peak is revealed in Fig. 2. The relaxation observed for a polycrystalline sample is insensitive for longitudinal excitation to both the $\langle 100 \rangle$ and $\langle 001 \rangle$ directions of tetragonal ZrO_2 .

3.3. $\langle 111 \rangle$ -oriented crystals

Fig. 3 shows E and Q^{-1} for a $\langle 111 \rangle$ -oriented sample of a crystal. A large internal-friction peak and an elastic anomaly were observed at around 300 °C. The loss amplitude at maximum was 2.0×10^{-2} , which is 1.4 times that for the polycrystalline samples, whereas the half-width for the single crystal was slightly smaller (0.60 K^{-1}) than for the polycrystals (0.61 K^{-1}). However, the relaxation peak is calculated to be 2.2 times broader than a single Debye peak using τ_0 and H obtained from an Arrhenius equation for polycrystalline samples. The results show the distribution of the relaxation time, i.e. complex relaxation processes in both crystalline and polycrystalline samples.

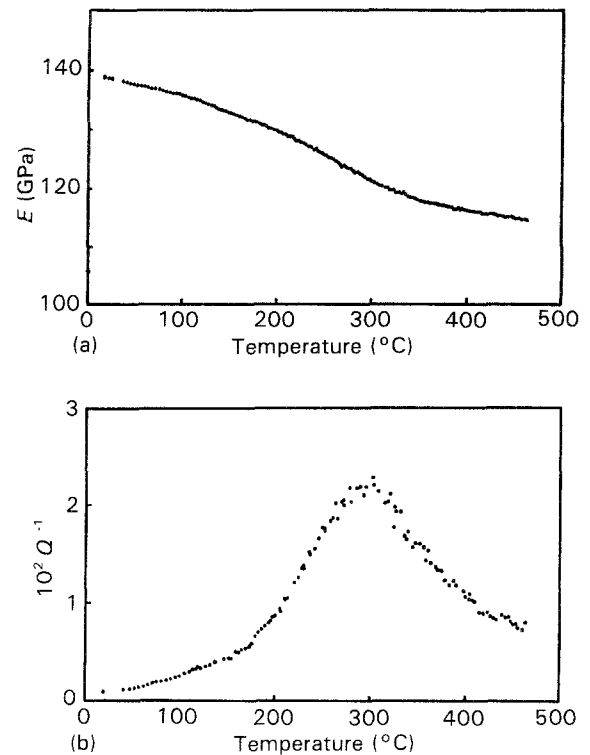


Figure 3 Temperature dependence of: (a) Young's modulus, E , and (b) internal friction, Q^{-1} , for a $\langle 111 \rangle$ -oriented 4 wt % Y_2O_3 - ZrO_2 crystal.

4. Discussion

4.1. Amplitude of relaxation

The relaxation amplitude of elastic compliance is discussed for $\langle 100 \rangle$ -oriented and $\langle 111 \rangle$ -oriented crystals and a polycrystalline body with cubic symmetry. The reciprocal Young's modulus, i.e. the tensile

compliance of a crystal, in an arbitrary direction is expressed by the principal compliance constants, s_{11} , s_{12} and s_{44} for a cubic system. There is an advantage to using three constants, following [11, 19].

$$\begin{aligned} s &= s_{44} \\ s' &= 2(s_{11} - s_{12}) \\ s'' &= s_{11} + 2s_{12} \end{aligned} \quad (1)$$

where, s is the shear compliance for a shearing stress applied across the (100) plane in the [010] direction, s' is the shear compliance for a shearing stress across the (110) plane in the [1 $\bar{1}$ 0] direction and s'' is one-third of the hydrostatic compressibility. The tensile compliance, J , in any direction of the crystal is given by

$$J = \frac{(s' + s'')}{3} - (s' - s)\Gamma \quad (2)$$

where, $\Gamma = (\xi_1\xi_2)^2 + (\xi_2\xi_3)^2 + (\xi_3\xi_1)^2$, and ξ_i are the directional cosines between the stress direction and the cubic axes. For the stress in the $\langle 100 \rangle$ direction, $\Gamma = 0$, and $\Gamma = 1/3$ for the $\langle 111 \rangle$ stress. The relaxation of the compliance is given by $\delta J = J_r - J_u$, where J_r and J_u are the relaxed and unrelaxed compliances, respectively. In the absence of reduction of the defect complexes, there is no hydrostatic relaxation ($\delta s'' = 0$). Thus, for the $\langle 100 \rangle$ and $\langle 111 \rangle$ directions, the amplitude of relaxation is given by

$$\delta J_{\langle 100 \rangle} = \frac{1}{3} \delta s' \quad (3)$$

$$\delta J_{\langle 111 \rangle} = \frac{1}{3} \delta s \quad (4)$$

Equations 3 and 4 indicate that the elastic measurements in the $\langle 100 \rangle$ and $\langle 111 \rangle$ orientations give the relaxation of the two principal shear compliances, s' and s .

The relation between Young's modulus, E ($= J_{\text{poly}}^{-1}$), shear modulus, G , and bulk modulus, K ($= (s'')^{-1}/3$), for a homogeneous body is described by

$$E^{-1} = \frac{K^{-1}}{9} + \frac{G^{-1}}{3} \quad (5)$$

Using the Reuss's shear modulus, $G^{-1} = (4s' + 3s)/5$ for a polycrystalline aggregate of cubic crystals [20, 21], J_{poly} is given by

$$J_{\text{poly}} = \frac{1}{3} s'' + \frac{4}{15} s' + \frac{1}{5} s \quad (6)$$

The relaxation amplitude is obtained by

$$\delta J_{\text{poly}} = \frac{4}{15} \delta s' + \frac{1}{5} \delta s \quad (7)$$

The experimental observations in the present study show no relaxation in the $\langle 100 \rangle$ -oriented crystal for either Young's modulus or the internal friction. Thus,

$$\delta s' = \delta (s_{11} - s_{12}) = 0 \quad (8)$$

The relaxation is only valid for δs , i.e. for δs_{44} . A large relaxation in Young's modulus was observed experimentally only for the $\langle 111 \rangle$ -oriented crystal. The relaxation amplitude should correspond to $\delta s_{44}/3$ quantitatively. On the other hand, the relaxation amplitude, δJ_{poly} , can be obtained for a polycrystalline body by applying $\delta s' = 0$ to Equation 7. Consequently, the

relaxation amplitudes for $\langle 111 \rangle$ -oriented, crystalline and polycrystalline samples are summarized as follows,

$$\begin{aligned} \delta J_{\langle 111 \rangle} &= \frac{1}{3} \delta s_{44} \\ \delta J_{\text{poly}} &= \frac{1}{5} \delta s_{44} \end{aligned} \quad (9)$$

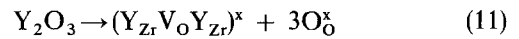
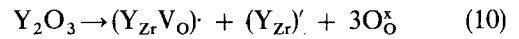
The ratio, $\delta J_{\langle 111 \rangle}/\delta J_{\text{poly}}$, is 1.67 theoretically.

In this study, the relaxation was measured as a function of temperature. Assuming a linear dependence of compliance on temperature, we obtain the relaxation amplitude of the compliance: $\delta J_{\langle 111 \rangle} = 6.7 \times 10^{-12} \text{ m}^2 \text{ N}^{-1}$, for a $\langle 111 \rangle$ -oriented crystal; and $\delta J_{\text{poly}} = 4.2 \times 10^{-12} \text{ m}^2 \text{ N}^{-1}$ for a polycrystalline body. The ratio of the relaxation amplitude for single crystals and the present polycrystalline samples was 1.6 experimentally. Considering that the relaxation amplitude also depends on the concentration of oxygen vacancies, which corresponds to the amount of doped Y_2O_3 , the ratio 1.67 should be increased to 1.88. The experimental result, 1.6, has a good consistency with the calculated value, 1.88, within the experimental error in the measurement.

4.2. Defect complex

The internal-friction peaks in the present study were broader than a single Debye relaxation. The results indicated that complex relaxation processes exist in both crystalline and polycrystalline aggregates. The relaxation due to a defect complex with certain symmetries in a crystal has been discussed by Nowick [13], Watchman [22] and others [23]. Nowick has described the selection rule for the anelastic and dielectric relaxation due to a defect complex with a dipole in a crystal.

When Y^{3+} cations substitute for Zr^{4+} and introduce oxygen vacancies, V_O , to compensate for charge, one V_O is produced for every Y_2O_3 in ZrO_2 . Homogeneous doping of Y_2O_3 will induce a local structure including a $(\text{Y}_\text{Zr}\text{V}_\text{O})'$ complex in a ZrO_2 lattice. However, inhomogeneous distribution of Y cations will lead to clustered defect complexes such as the triplet $(\text{Y}_\text{Zr}\text{V}_\text{O}\text{Y}_\text{Zr})$. The latter situation is expected in ZrO_2 samples with a large amount of Y_2O_3 doping. These reactions are described by the following Kröger-Vink notation



The defect complex $(\text{Y}_\text{Zr}\text{V}_\text{O})'$ is a pair consisting of a centred cation and a co-ordinated oxygen vacancy with eight equivalent sites (type I). The complex $(\text{Y}_\text{Zr}\text{V}_\text{O}\text{Y}_\text{Zr})^\times$ is classified into two cases: two Y^{3+} cations are arranged along cubic axes and one V_O is co-ordinated by both Y^{3+} cations (type II), and two Y^{3+} are arranged along the $\langle 111 \rangle$ direction and one V_O is co-ordinated by a Y^{3+} cation (type III). These defect structures are the same as those in fluorite-type CeO_2 doped with 0.5, 1 and 2 wt % Y_2O_3 , which have been discussed by Anderson and Nowick [24]. In their experiments a single Debye peak was observed for

0.5 wt % Y_2O_3 - CeO_2 ; however, a broad internal-friction peak appeared for 1 wt % and 2 wt % Y_2O_3 - CeO_2 . The results indicated that CeO_2 with large amounts of Y_2O_3 contained two or more complexes as the cause of a relaxation. The selection rule, discussed for CeO_2 - Y_2O_3 , shows that δs_{44} is valid and that $\delta(s_{11}-s_{12}) = 0$ for a pair ($Y_{Zr}V_O$) with trigonal symmetry to the $\langle 111 \rangle$ axis. Furthermore, for the triplet ($Y_{Zr}V_O Y_{Zr}$), the relaxation is also active on s_{44} and inactive on $(s_{11}-s_{12})$, if no Y^{3+} cations move in the relaxation process. The diffusion of oxygen or oxygen vacancies is very fast and cations have low mobility in ZrO_2 at moderate temperatures. Thus, these complexes can become a cause of anelastic relaxation for the compliance s_{44} , but not for $(s_{11}-s_{12})$.

The complicated relaxations, giving distributed relaxation time and enthalpy, are considered to be induced by following causes for the ZrO_2 crystal used in this study.

1. The ZrO_2 used has no cubic symmetry but has a small tetragonality, $c/a = 1.015$. The relaxation jump of oxygen vacancies along the a -axis or the c -axis occurs with slightly different frequencies due to the different distances of neighbouring oxygen sites between the two axes' directions.

2. The defect complexes of types I, II and III are expected as the causes of δs_{44} -type relaxation. It is believed that the interactions of cation-vacancy, such as $Y^{3+}-V_O$, $Zr^{4+}-V_O$, and their variations under different surrounding situations, induce the distribution of relaxation time and enthalpy for relaxations.

5. Conclusion

Mechanical relaxation was examined in polycrystals and crystals with orientations in the $\langle 100 \rangle$ and $\langle 111 \rangle$ directions. The relaxation was observed for $\langle 111 \rangle$ -oriented crystals, but not for $\langle 100 \rangle$ -oriented crystals. The results indicated that the relaxation was active only for s_{44} , being inactive for $(s_{11}-s_{12})$. The amplitude of anelastic relaxation is calculated on polycrystalline and $\langle 111 \rangle$ -crystal bodies. The Experimental data had a good consistency with the values calculated from Equations 1-11. A broad relaxation peak indicated that complex processes exist even crystals. Possible defect complexes were discussed, and a pair and triplets were expected to be active for the present relaxation.

Acknowledgement

We would like to thank Mr Tatsuo Noritake for help in preparing the oriented crystals.

References

1. B. C. H. STEELE, J. H. BECHTOLD, R. K. SLOTWINSKI, N. BONANOS and E. P. BUTLER, *Adv. Ceram.* **3** (1981) 286-309.
2. D. J. GREEN, R. H. J. HANNINK and M. V. SWAIN, "Transformation toughening", (CRC Press, Boca Raton, USA 1989).
3. T. SATO, S. OHTAKI, T. ENDO and M. SHIMADA, *Adv. Ceram.* **24** (1988) 29-37.
4. K. MATSUSHITA, T. OKAMOTO and M. SHIMADA, *J. Phys. (Paris) C* **10** (suppl, 1985), 549-552.
5. M. WELLER and H. SCHUBERT, *J. Amer. Ceram. Soc.* **69** (1986) 573-77.
6. S. SAKAGUCHI, F. WAKAI and S. MATSUNO, *J. Ceram. Soc. Jpn.* **95** (1987) 476-79.
7. K. NISHIYAMA, M. YAMANAKA, M. OMORI and S. UMEKAWA, *J. Mater. Sci. Lett.* **9** (1990) 526-8.
8. M. OZAWA, T. HATANAKA and H. HASEGAWA, *J. Mater. Sci. Lett.* **10** (1991) 774-5.
9. M. OZAWA, T. HATANAKA and H. HASEGAWA, *J. Ceram. Soc. Jpn.* **99** (1991) 643-8.
10. A. S. NOWICK, "Point defect in solids", Vol. 1, edited by J. H. Crawford and L. M. Sliifkin (Plenum Press, New York, 1972) Ch. 3, pp. 151-200.
11. A. S. NOWICK and W. R. HELLER, *Adv. Phys.* **12** (1963) 251-298.
12. *Idem., ibid.* **14** (1965) 101-166.
13. A. S. NOWICK, *Adv. Phys.* **16** (1967) 1-47.
14. J. ZACHARIAS, *Phys. Rev.* **49** (1936) 50-54.
15. T. IKEDA, "Fundamentals of piezoelectric materials science", (Oxford University Press, London, 1990).
16. S. KUDO and M. OZAWA, *Jpn. J. Appl. Phys.* **28** (suppl. 2, 1989) 184-6.
17. M. OZAWA and S. KUDO, *J. Ceram. Soc. Jpn.* **98** (1990) 987-90.
18. J. W. ADAMS, H. H. NAKAMURA, R. P. INGEL and R. W. RICE, *J. Amer. Ceram. Soc.* **68** (1985) C 228-31.
19. C. ZENER, *Phys. Rev.* **71** (1947) 34.
20. A. REUSS, *Z. Angew. Math. Mech.* **9** (1929) 49.
21. Z. HASHIN and S. SHTRIKMAN, *J. Mech. Phys. Solids.* **10** (1962) 343-352.
22. J. B. WACHTMAN, *Phys. Rev.* **131** (1963) 517-27.
23. R. W. DREYFUS and R. B. LAIBOWITZ, *Phys. Rev. A* **135** (1964) 1413-22.
24. M. P. ANDERSON and A. S. NOWICK, *J. Phys. (Paris) C* **5** (suppl. 1981) 823-28.

Received 3 July 1992

and accepted 25 February 1993